

Parametric Simulation Framework for Cycloidal Gear Actuators Using ANSYS and RecurDyn

Feng MIAO, Junhua BAO*

Abstract: This study introduces an integrated parametric simulation framework utilizing ANSYS and RecurDyn for the performance evaluation and design optimization of cycloidal gear actuators. The proposed framework synergizes Finite Element Analysis (FEA) and Multi-Body Dynamics (MBD) simulations, effectively overcoming the limitations inherent in traditional isolated analyses, where static stress distribution and dynamic behavior are typically modeled separately. Unlike conventional methods, which often lack flexibility and real-time adjustments, the hybrid approach presented in this paper enables automated parameter updates, significantly enhancing design optimization processes and fatigue life prediction accuracy. The methodology is comprehensively outlined, covering all stages from model generation and mesh refinement to load application and fatigue life prediction. This detailed workflow illustrates the framework's robust capability in simulating and optimizing gear performance. Additionally, a broad range of visual outputs, including contact stress contour plots, transmission error curves, and vibration frequency domain data, is provided, offering a holistic view of the system's performance. While the technical approach is thorough, this work identifies critical gaps in current simulation tools, specifically the lack of automation and integrated dynamic modeling. The proposed ANSYS-RecurDyn platform addresses these challenges, providing a flexible and efficient tool for real-time parameter adjustments. The framework's implementation has significant implications for applications in fields such as robotics, aerospace, and precision machinery, where high torque efficiency and fatigue reliability are essential.

Keywords: cycloidal gear actuators; fatigue life prediction; finite element analysis; gear optimization; parametric simulation

1 INTRODUCTION

Cycloidal gear actuators are widely utilized in robotics, aerospace, precision machinery, and industrial automation due to their high reduction ratios, compact design, and excellent torque transmission efficiency [1]. Compared to planetary and harmonic drives, cycloidal reducers offer low backlash, high torsional stiffness, and shock resistance, making them ideal for applications that require precise motion control and high-load transmission [2]. However, their complex meshing characteristics, sensitivity to dimensional errors, and nonlinear dynamic behaviour pose significant challenges in design optimization and performance evaluation [3]. The efficiency and longevity of cycloidal gear actuators are highly influenced by manufacturing precision, contact stresses, and friction losses, which necessitate an advanced approach to simulation, optimization, and predictive analysis [4].

Traditional analysis methods rely on empirical formulas, experimental validation, and simplified finite element analysis (FEA) to study stress distribution, deformation, and failure mechanisms [5]. However, these approaches have several limitations. FEA-based static analysis often fails to capture the transient interactions and dynamic effects of real-world operational conditions, leading to inaccuracies in fatigue life prediction [6]. Similarly, multi-body dynamics (MBD) simulations have been widely used to assess kinematic behavior, transmission errors, and vibration characteristics, yet conventional MBD models often oversimplify gear contact interactions, resulting in discrepancies between simulation and actual performance [3]. Furthermore, manual parameter adjustments in gear optimization remain time-consuming and inefficient, highlighting the need for an automated and integrated simulation framework [4].

Recent advancements in computational modeling have introduced parameterized FEA and MBD integration, enabling more accurate predictions of stress-strain

distributions, meshing efficiency, and fatigue failure mechanisms [6]. Studies have explored the impact of dimensional errors on cycloidal gear performance, revealing that even minor deviations can significantly influence torque ripple, meshing characteristics, and energy losses [2]. Moreover, researchers have investigated novel tooth profile designs, such as epitrochoidal modifications and non-pin roller mechanisms, which aim to enhance operational stability and reduce stress concentrations [5]. Additionally, multi-objective optimization techniques, including genetic algorithms, have been employed to refine load distribution strategies and minimize friction-induced wear [7].

A key focus in recent research is fatigue life assessment through finite element dynamic simulation. The integration of wear prediction models with FEA and MBD has improved long-term durability analysis and enhanced the understanding of contact fatigue and cyclic stress accumulation in cycloidal reducers [3]. Despite these advancements, existing research lacks a fully automated and integrated simulation approach that enables real-time parametric adjustments, transient dynamic analysis, and friction loss optimization [6].

This study aims to bridge these gaps by developing a Parameterized Simulation Calculation Specification for Cycloidal Gear Actuators using ANSYS APDL and RecurDyn. The proposed methodology integrates FEA for structural stress analysis and MBD for dynamic behavior evaluation, allowing for automated parameter adjustments and real-time performance assessment. The primary objectives of this research include:

- Enhancing the accuracy of stress-strain evaluations to improve fatigue life prediction.
- Developing a robust dynamic modeling approach to capture transmission errors, torsional stiffness variations, and load distribution effects.
- Optimizing gear contact interactions to minimize energy losses and friction-induced wear, thereby increasing overall efficiency.

- Establishing an automated simulation framework that integrates fatigue life assessment and multi-objective optimization to improve design iteration efficiency.

By combining advanced computational modeling with automated parametric optimization, this research presents a systematic and practical approach to optimizing cycloidal gear actuators. The findings of this study will have significant implications for robotics, aerospace, and precision engineering, enabling more efficient and durable high-performance transmission systems [8, 9].

Despite the widespread use of cycloidal gear reducers, existing simulation approaches often lack automation and fail to integrate dynamic response with structural evaluation. These limitations hinder efficient design iteration and performance optimization.

To address these gaps, this study proposes a parametric simulation framework that integrates finite element analysis (FEA) and multi-body dynamics (MBD) via ANSYS and RecurDyn. The framework enables automatic parameter control, dynamic-static coupling, and fatigue life prediction - providing a comprehensive tool for efficient and reliable design of high-performance cycloidal gear actuators.

2 APDL MODELING AND ASSEMBLY OF CYCLOIDAL ACTUATORS

2.1 Simulation Framework Overview

The computational framework developed in this study integrates ANSYS APDL and RecurDyn within a modular architecture. ANSYS is employed for geometric modeling, mesh generation, and static finite element contact analysis, while RecurDyn is utilized for dynamic system construction, automated model updating, and dynamic response and sensitivity analysis. Upon completion of the mesh model - parametrically controlled via APDL - the finite element components in the existing RecurDynPNet dynamic model are programmatically updated. Subsequently, the relevant kinematic pairs and load conditions are redefined, and a new simulation model is constructed for analysis and result extraction.

The ANSYS modeling process is organized into distinct modules, including the external cycloidal gear, internal cycloidal gear, and output disk. Each module is independently defined, equipped with a dedicated parameter input interface, and generates a corresponding *.cdb model file upon parameter specification [10].

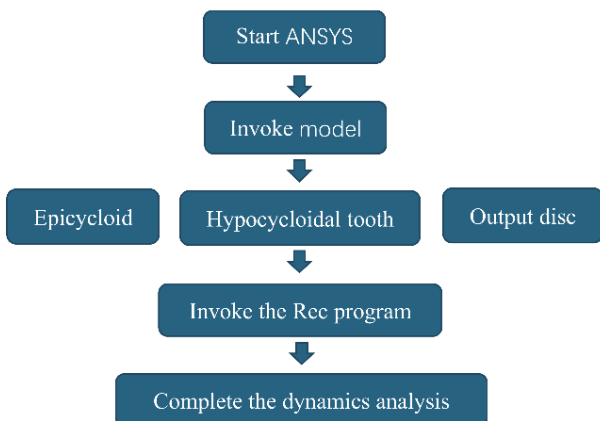


Figure 1 ANSYS-APDL & RecurDyn calculation program block diagram

The execution process of the simulation workflow is illustrated in Fig. 1. Initially, a model subroutine is invoked to generate the finite element *.cdb files for each of the aforementioned modules. These model files are subsequently imported into RecurDyn via the PNet interface, where they are assembled, spatially aligned, and assigned appropriate kinematic pairs, constraints, and loading conditions. The simulation is then executed, culminating in dynamic analysis and fatigue life evaluation.

2.2 Finite Element Model Modeling

Based on the specified design parameters and technical drawings, parametric models of the external cycloidal gear, internal cycloidal gear, and output disk were constructed to represent the core components of the cycloidal reducer. Representative examples of the parameter input interface and corresponding APDL program scripts are shown in Fig. 2.

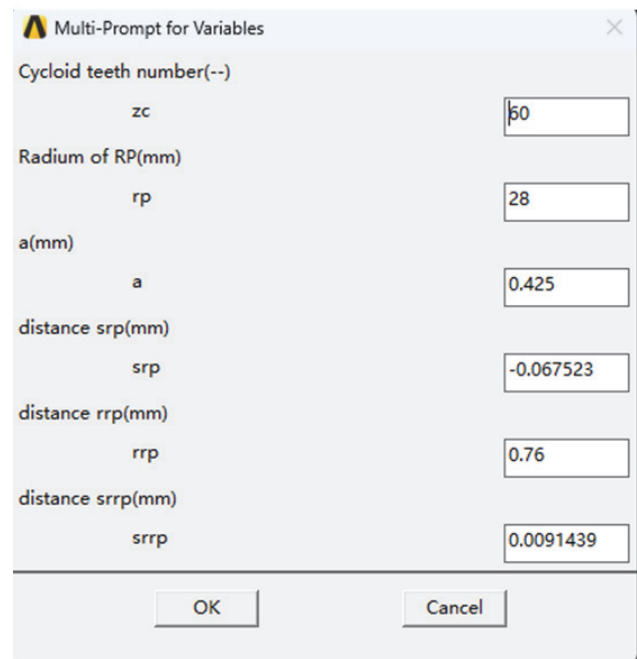


Figure 2 Pendulum structure parameter input interface

To ensure both transmission precision and structural reliability, the selection of key geometric parameters was not limited to achieving the target reduction ratio but also considered their influence on load-bearing capacity, dynamic response, and sensitivity to manufacturing tolerances. Specifically, the number of teeth z_c was selected based on the required transmission ratio, which directly determines the reduction stage and meshing frequency. The eccentricity a , which controls the amplitude of the cycloidal motion, was optimized to strike a balance between system stiffness and dynamic stability, thereby minimizing vibration and displacement error.

Furthermore, recent studies such as Yang et al. [11] and Cheng et al. [12], have highlighted the nonlinear influence of geometric deviations and clearance parameters - such as s_{rp} and s_{rrp} - on contact stiffness, transmission efficiency, and fatigue reliability. Guided by these findings, the parameter configuration adopted in this

study follows a reliability-based design approach, incorporating insights from tooth profile modification, rolling pin geometry optimization, and tolerance allocation strategies to enhance robustness and manufacturability.

As shown in the parameter input interface, the mechanical behavior of the cycloidal drive is governed by a set of core design variables. The variable z_c specifies the number of teeth (or pins) in the cycloidal gear, which determines the reduction ratio and meshing rhythm. r_p represents the radial distance to the center of the pin gear, affecting both the torque transmission path and contact geometry. a denotes the eccentricity, which defines the amplitude of the cycloidal motion and significantly influences vibration characteristics. s_{rp} is the displacement correction factor for the cycloidal wheel, enabling fine adjustment of the contact point positions. r_{rp} defines the radius of the rolling pin sleeve, which governs rolling efficiency and load capacity. Finally, s_{rrp} represents the radial clearance between rolling pins and their mating holes, a critical parameter affecting backlash, meshing stability, and long-term fatigue wear.

An excerpt of the APDL script used to define and input these parameters programmatically is provided below. This segment highlights how the modular interface enables direct assignment of variable values for flexible and automated simulation configuration:

```
!***** Input hub and spoke
parameters *****
multipro,'start',6
*cset,1,3,zc,'Cycloid teeth number(--)',60 ! Cycloidal
gear tooth number
*cset,4,6,rp,'Radium of RP(mm)',28 ! Pin gear
center radius
*cset,7,9,a,'a(mm)',0.425 ! Eccentricity
*cset,10,12,srp,'distance srp(mm)',-0.028149 !
Cycloidal wheel displacement modification
*cset,13,15,rrp,'distance rrp(mm)',0.76 ! Pin gear
sleeve radius
*cset,16,18,srrp,'distance srrp(mm)',0.022216 !
Cycloidal wheel equal-distance modification
multipro,'end'
```

This code snippet reflects the modular structure of the APDL-based modeling system, allowing each parameter to be independently adjusted through a structured input interface, thereby enhancing simulation flexibility and repeatability. Specifically, the script utilizes the `multipro` and `*cset` commands to define key geometric parameters of the cycloidal gear system, including the number of cycloidal teeth (z_c), the radius to the pin gear center (r_p), the eccentricity (a), the displacement modification of the cycloidal wheel (s_{rp}), the sleeve radius of the pin gear (r_{rp}), and the equal-distance adjustment parameter (s_{rrp}). Each parameter is input with an assigned index and accompanied by a descriptive label and unit, enabling clear physical interpretation and seamless integration into the simulation workflow. This structured approach supports efficient parametric modeling, sensitivity analysis, and automated multi-scenario simulation.

2.3 Model Generation

In this study, the `*use` macro call command in APDL is employed for model generation, during which relevant

parameters are defined and input at the call stage. To avoid potential conflicts caused by parameter interactions across modules, the `*clear` command is executed after each `*use` call to remove existing parameters and models, ensuring that the basic parameters of the tooth profile remain consistent throughout the process. Notably, the rationality of parameter configuration is not only derived from engineering experience but also informed by the systematic study conducted by Zhang et al. [13]. Their work established a theoretical model for evaluating the bearing capacity of cycloid-pin gear mechanisms, quantifying the influence of key design parameters such as eccentricity, pin gear distribution radius, number of pin teeth, and gear thickness on the load distribution coefficient, maximum contact stress, and overall torsional stiffness. Furthermore, their theoretical results were validated through finite element simulations, confirming the effectiveness of parameter optimization strategies. This provides solid theoretical support and optimization guidance for the parameter setting in the model generation module of this study.

2.4 Modeling and Setting of Rigid-flexible Coupling Dynamic Model

The initial RecurDyn model is manually constructed by defining the basic geometry, kinematic pairs, and loading conditions between components. Once the base structure is complete, the PNet module is employed to replace rigid parts with finite element models corresponding to different parameter configurations. This enables automated generation of a fully integrated rigid-flexible dynamic model.

Model import and assembly alignment:

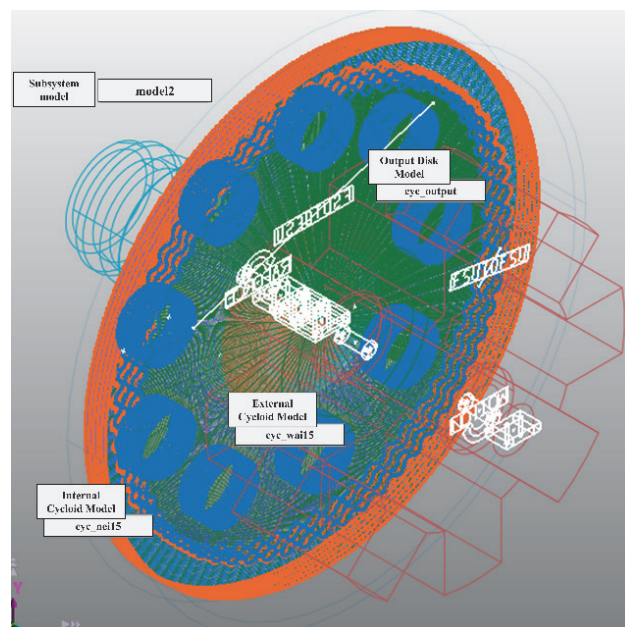


Figure 3 Model import and finite element setting parameter input interface

As illustrated in Fig. 3, the model components - including the external cycloidal gear, internal cycloidal gear, and output disk - are primarily defined with the global coordinate origin as the reference. Therefore, appropriate translation and rotational alignment must be applied during the import process. Parameter input is conducted via the

graphical interface shown above, where users specify the file path and name of each *.cdb file. Once confirmed, clicking the "Import" button integrates the component into the simulation environment with the correct spatial configuration.

Finite element model setting:

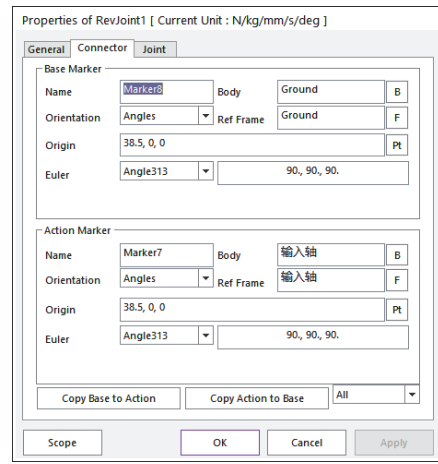
After mesh generation, loads, boundary constraints, coupling conditions, and contact pairs are applied, as shown in the parameter input panels. The mesh scale is defined as follows: the internal cycloidal gear consists of 25,622 nodes and 17,082 elements; the external cycloidal gear comprises 120,461 nodes and 99,749 elements; the output disk includes 12,866 nodes and 9,102 elements. In total, the assembled model contains 158,949 nodes and 125,933 elements.

Fixed Connection Setup:

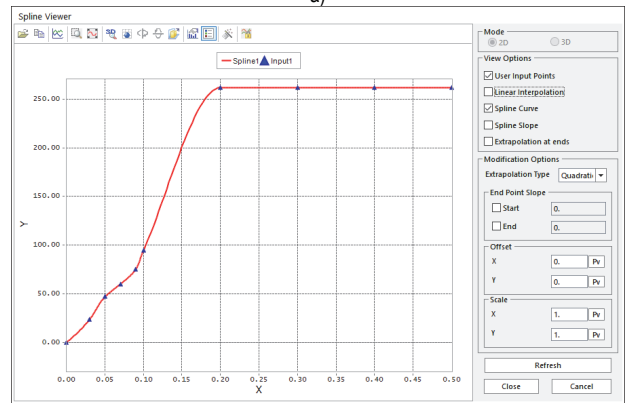
- Two fixed supports are established between the internal cycloidal gear and the frame, constraining the needle gear movement.

Contact Pairs:

- Contact pair between the internal cycloidal gear and the external cycloidal gear.
- Contact pair between the pin on the cycloidal wheel and the output disk.

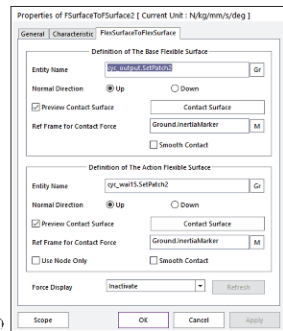
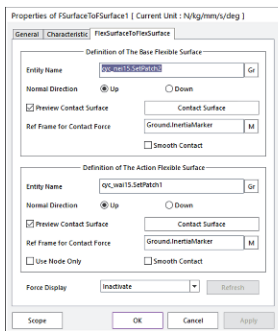


a)



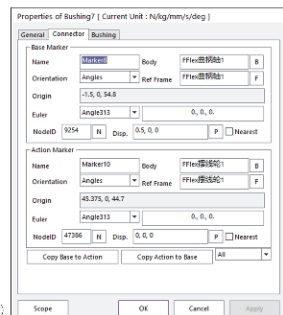
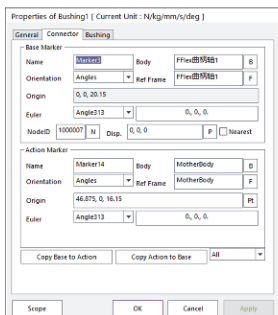
b)

Figure 5 Revolute joint and load parameter setting interface; a) Input shaft revolute pair; b) Input shaft speed curve



a)

b)



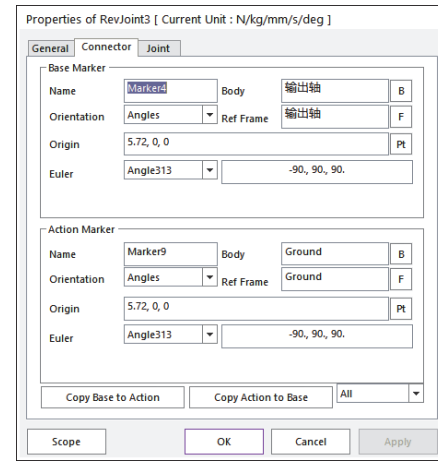
c)

d)

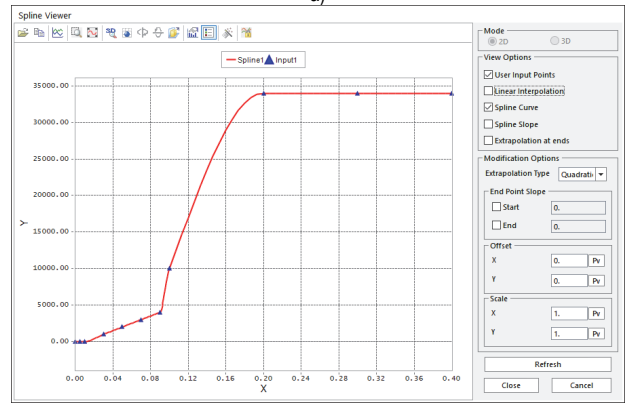
Figure 4 Bearing pair parameter setting interface: a) Central wheel and planetary wheel; b) Cycloidal wheel and pin wheel; c) Crankshaft and planetary carrier; and d) Cycloidal wheel and crankshaft

Revolute Pairs:

- Establish the revolute pair relationship between the crankshaft and the frame, and apply the input rotational speed.
- Establish the revolute pair relationship between the output disk and the frame, and apply the output torque load.
- The revolute joint relationship between the outer cycloidal gear and the input crank shaft.



a)



b)

Figure 6 Revolute joint and load parameter setting interface; a) Input shaft revolute pair; b) Load torque curve

3 EXAMPLES OF ANSYS AND RecurDyn SIMULATION ANALYSIS RESULTS

3.1 ANSYS Analysis Results

The modeling and static simulation of the cycloidal drive mechanism were conducted using APDL scripting within ANSYS. The generated finite element model is illustrated in Fig. 7.

As shown, the outer surface nodes of the internal cycloidal gear are fully constrained. The output pin disk is subjected to radial and axial constraints while retaining circumferential degrees of freedom, and a torque of 30,000 N·mm is applied to its outer surface nodes. Radial and axial constraints are also applied to the inner bore of the external cycloidal gear. Contact pairs are defined between the internal and external cycloidal teeth, as well as between the pins of the cycloidal gear and the corresponding holes on the output disk. These boundary and contact conditions simulate the static contact behavior of the output mechanism under the action of the applied torque T_2 .

The model consists of 443,706 nodes and 408,180 elements, reflecting a high-resolution mesh suitable for capturing detailed stress and contact interactions.

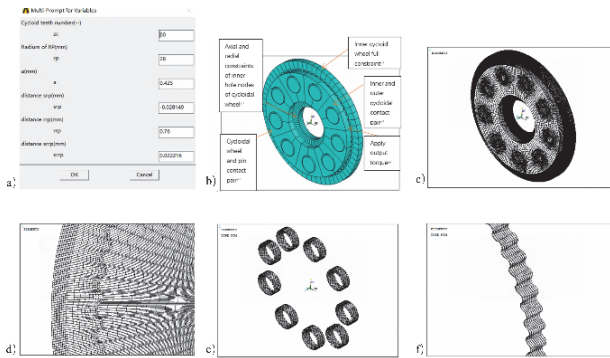


Figure 7 Finite element model of transmission device: a) Simulation parameter input interface; b) Model simulation settings; c) Finite element model (output side); d) Internal and external cycloidal teeth (input side); e) Output pin contact pair; and f) Internal and external cycloidal teeth contact pair

According to the above calculation parameters, through the finite element analysis, the results are as follows:

(a) Contact strength: The contact stress of cycloidal wheel is about 563 MPa, and the contact stress is about 426 MPa, both of which are less than the ultimate stress of the material;

The simulation results of structural design are shown in Fig. 8.

3.2 RecurDyn Dynamics Simulation Analysis Results

Recent research has highlighted the significant impact of tooth profile modifications and system errors on the dynamic behavior and transmission precision of cycloidal reducers, with studies such as Yang et al. (2021) developing advanced dynamic models to assess these factors [14].

Transmission ratio:

The simulation duration for the trial calculation was 0.4 seconds, with 4,000 steps. The average output shaft speed within the 0.2-0.4 seconds after the speed stabilized was 4.38 rad/s. The average transmission ratio of the simulation model was calculated to be 59.77, with a transmission ratio error of approximately 0.38%. The

simulation results accurately replicated the operating conditions of the transmission device.

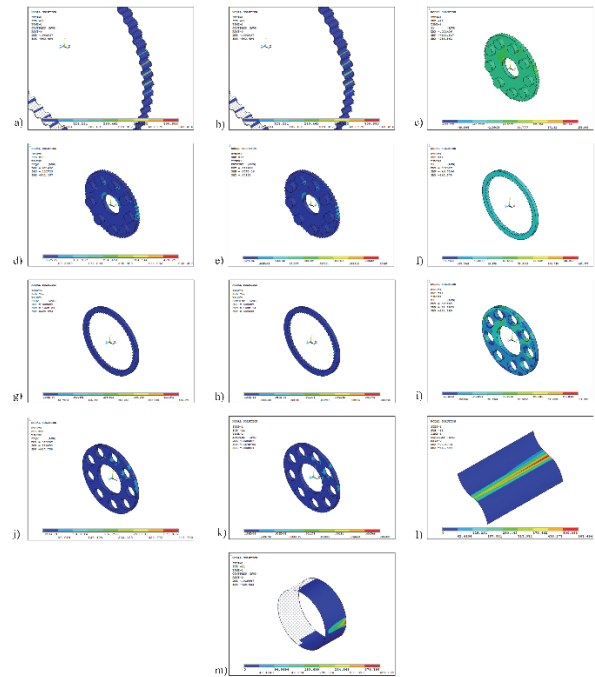


Figure 8 Stress contour plot highlighting high-stress concentrations, indicating potential fatigue failure points: a) Cycloidal tooth contact stress contour plot; b) Pin contact stress contour plot; c) First principal stress contour plot; d) Equivalent stress contour plot; e) Total strain contour plot; f) First principal stress contour plot; g) Equivalent strain contour plot; h) Strain contour plot; i) First principal stress contour plot of the output disk; j) Equivalent stress contour plot of the output disk; k) Equivalent strain contour plot of the output disk; l) Cycloidal wheel tooth contact stress plot; and m) Output pin contact stress contour plot

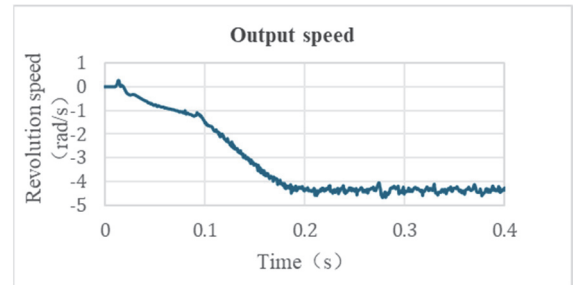


Figure 9 Speed change curve

Transmission error:

The input shaft and output shaft angles within the 0.2-0.4 seconds of the simulation analysis, where the speed stabilized, were processed to determine the fluctuation range of the transmission error, as shown in the figure below. Under the simulation conditions without considering factors such as bearing clearance, bearing deformation, etc., the average calculated transmission error is approximately 1.78'.

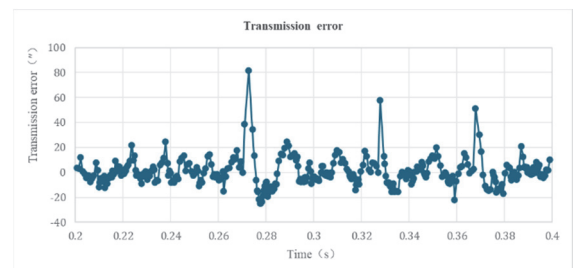


Figure 10 Transmission error curve

Backlash:

The transmission device backlash can be analyzed by setting the forward and reverse process of the model, which can be completed in the follow-up work.

Vibration characteristic analysis:

The dynamic characteristics of the transmission device can be analyzed by extracting the calculated data.

By extracting the angular acceleration curve in the transmission process and performing FFT transform, the vibration response of the whole machine can be obtained, as shown in the figure. The frequency range that affects the dynamic performance of the whole machine can be determined from the FFT curve.

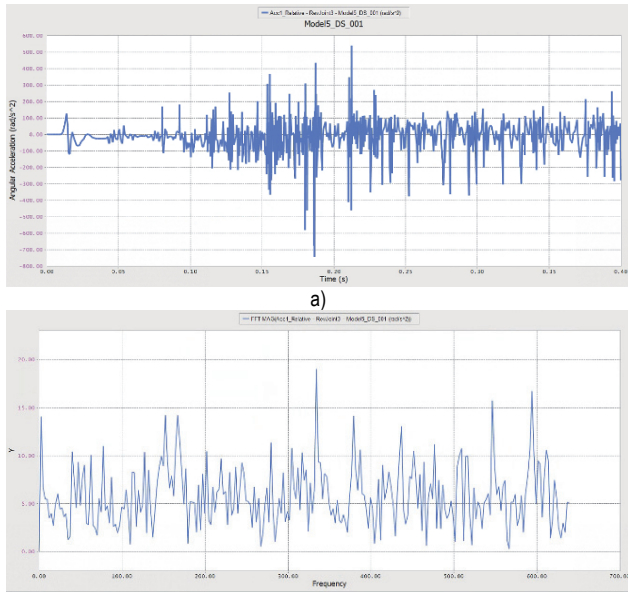


Figure 11 Acceleration curve; a) Output angular acceleration curve; and b) Angular acceleration frequency domain curve

Contact force:

From the calculation results, the real-time contact force changes between cycloidal wheels and between cycloidal wheels and column pins can be determined.

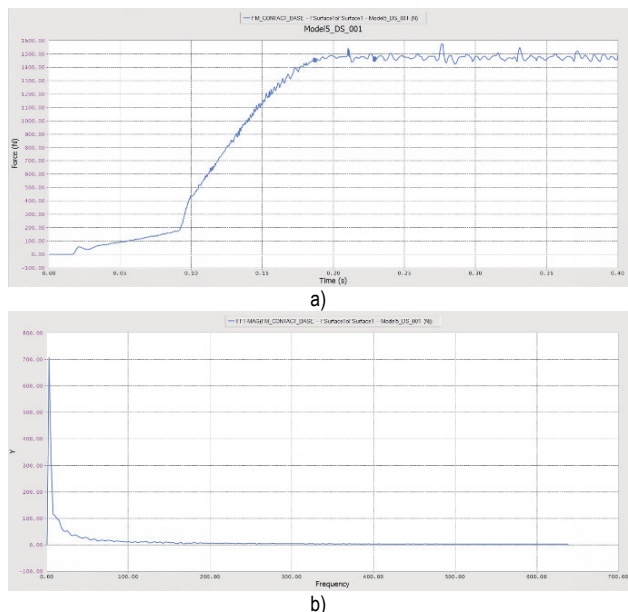


Figure 12 Cycloidal wheel contact force curve; a) time domain curve; and b) frequency domain curve

Fig. 12a shows the cycloidal wheel contact force variation in the time domain. Between 0 to 0.09 seconds, the contact force remains relatively stable with little change. However, from 0.09 to 0.18 seconds, the contact force sharply rises to approximately 1500 N. Following this, the contact force fluctuates steadily between 1450 N and 1550 N, with a smooth and relatively small amplitude, indicating that the gear meshing process is stabilizing. However, the sharp increase in contact force could indicate significant meshing impacts, which, if not controlled, could lead to gear wear and fatigue.

Fig. 12b presents the contact force in the frequency domain. In the frequency-domain curve, there is an initial sudden increase and sharp decrease in contact force, reflecting large shocks or instability during the initial stage of operation. Afterward, the curve gradually converges and approaches zero, indicating that high-frequency components of the contact force dissipate as the system stabilizes. This trend suggests that after the initial transient state, the gear meshing process becomes more stable, and the contact force fluctuations decrease.

In summary, the analysis of contact force variation in both the time and frequency domains provides essential insights into gear system behavior. By optimizing gear design, reducing backlash, and selecting appropriate materials, it is possible to effectively reduce contact force fluctuations and vibrations, thereby enhancing dynamic performance and extending the gear's service life.

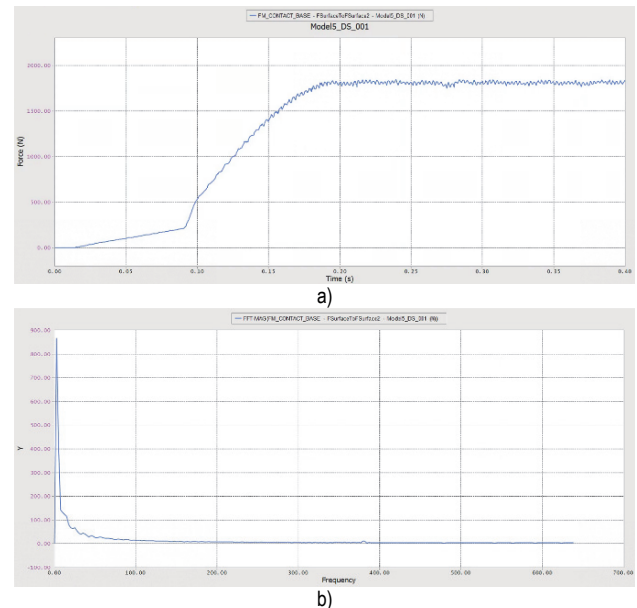


Figure 13 The change curve of contact force between cycloidal wheel pin and output disc; a) time domain curve; and b) frequency domain curve

In Fig. 13a, which shows the time-domain contact force variation, the contact force between the cycloidal wheel pin and the output disc remains relatively stable between 0 and 0.09 seconds, with minimal fluctuation. However, from 0.09 to 0.18 seconds, there is a sudden surge in contact force, followed by stabilization around 1800N with continued fluctuations. This behavior is similar to that observed in the previous contact force analysis but reflects the dynamic load changes specific to the interaction between the pin and the output disc. The rapid increase in force suggests a significant meshing event or a transition in the operational conditions, which may

lead to increased wear or potential fatigue issues if sustained.

Fig. 13b, showing the contact force in the frequency domain, also reveals a rapid increase and sharp decrease at the beginning of the curve. This indicates a transient dynamic behavior typical of the initial meshing impact. After this initial shock, the curve gradually decays towards zero, suggesting that the high-frequency components dissipate as the system stabilizes. This trend is similar to the previous frequency-domain analysis, reinforcing the notion that the system undergoes a transient state before settling into a more stable operational phase.

In conclusion, the analysis of contact force between the cycloidal wheel pin and output disc, both in time and frequency domains, further emphasizes the importance of managing dynamic load fluctuations. By optimizing gear meshing geometry, minimizing backlash, and selecting appropriate materials, it is possible to mitigate undesirable force spikes and vibrations, improving system stability and extending gear life.

Fatigue analysis and material selection justification:

To evaluate fatigue performance under high-load dynamic conditions, this study utilized 4340/243 steel as the reference material for simulation, due to its well-documented fatigue behavior and mechanical similarity to SUS420J2. Both steels are martensitic alloys with comparable tensile strength after heat treatment [15]. However, compared to SUS420J2 - which, despite its corrosion resistance and wear performance, lacks a distinct fatigue limit - 4340 steel exhibits higher endurance strength and more stable *S-N* behavior under cyclic stress [16, 17]. As shown in Fig. 14, the adopted *S-N* curve of 4340/243 steel demonstrates a clear fatigue limit suitable for high-cycle fatigue evaluation, enhancing the reliability of fatigue life predictions in this simulation.

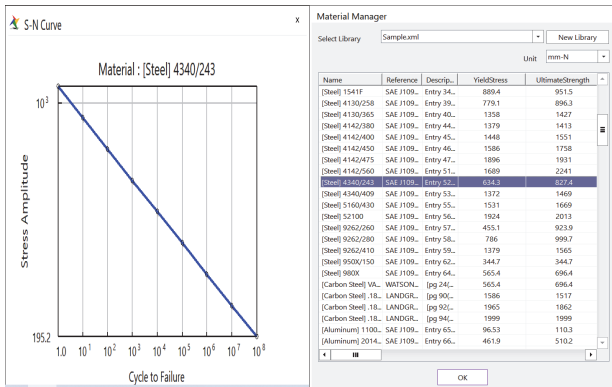


Figure 14 S-N curve of 4340/243 steel used for fatigue life prediction, showing a well-defined endurance limit suitable for high-cycle performance assessment

Moreover, recent metallurgical research confirms that quenched and tempered 4340 steel maintains a uniform martensitic microstructure with fine carbide dispersion, enabling consistent mechanical properties under severe fatigue and environmental exposure [16].

By contrast, SUS420J2 is more prone to surface-initiated fatigue failure and lacks the endurance strength required for long-term high-stress applications [15]. Hence, the use of 4340 steel as a surrogate material for fatigue simulation in this study is both mechanically justified and supported by safety considerations in engineering design. This substitution ensures conservative, repeatable fatigue

assessments while remaining representative of SUS420J2's general mechanical behavior.

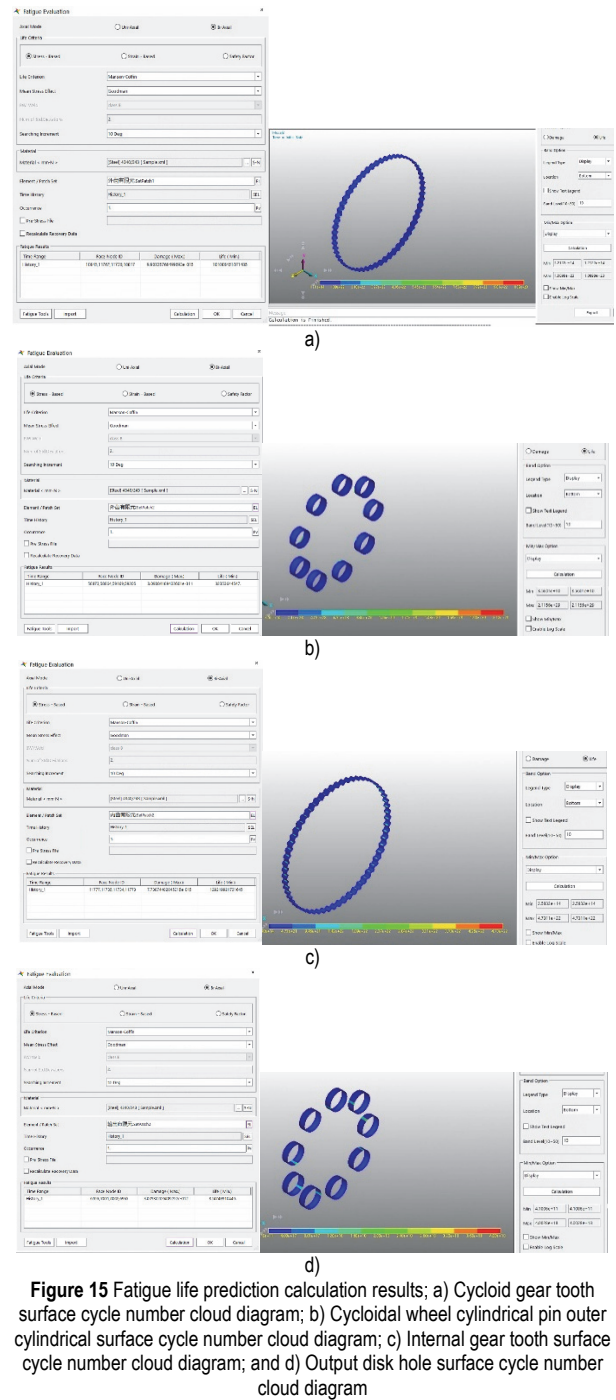


Figure 15 Fatigue life prediction calculation results; a) Cycloid gear tooth surface cycle number cloud diagram; b) Cycloidal wheel cylindrical pin outer cylindrical surface cycle number cloud diagram; c) Internal gear tooth surface cycle number cloud diagram; and d) Output disk hole surface cycle number cloud diagram

4 DISCUSSION

4.1 Stress Distribution Insights

The integrated FEA simulation results revealed that the contact stresses on both the cycloidal wheel and the pin remained significantly below the material's yield strength, indicating adequate structural safety under the applied torque load of 30,000 N·mm. The equivalent stress and strain fields also exposed localized stress concentrations, particularly near the root fillets and pin-hole interfaces. These zones serve as potential fatigue initiation points and should be given priority in structural refinement. The high-resolution mesh model, consisting of over 400,000

elements, ensured accurate representation of these critical regions.

In a comparative analysis of cycloidal and involute gear drives, Tariq et al. [18] observed that conventional cycloidal gear designs engage multiple radial contact points, leading to localized stress concentrations at the tooth fillets and pin-hole areas, consistent with the stress distribution observed in this study.

4.2 Dynamic Response Evaluation

Dynamic simulations conducted via RecurDyn demonstrated strong alignment with expected kinematic behavior. The system achieved an average transmission ratio error of only 0.38%, and transmission error fluctuations remained within 1.78 arcminutes under stable operating conditions. These results validate the model's fidelity in simulating real-world gear motion. Furthermore, frequency-domain analysis of angular acceleration revealed distinct resonance peaks, which provide valuable guidance for optimizing damping strategies and avoiding structural resonance.

4.3 Fatigue Behaviour and Lifetime Prediction

The integration of time-domain contact forces with material fatigue limits enabled a preliminary evaluation of the gear system's fatigue performance. Stress cycles observed in the contact regions - particularly in the cycloidal tooth flanks and pin holes - exhibited low amplitude and stable periodicity, suggesting favorable fatigue behavior. Although experimental validation is not included in this study, the simulation-based assessment offers a reliable basis for comparative life prediction.

4.4 Design Sensitivity and Clearance Trade-Offs

One of the key contributions of this framework lies in its automated parameter variation capability.

As shown in Fig. 16, the simulation explored the influence of different pin-to-hole clearances and tooth tip clearances on average transmission efficiency. The results demonstrate that minimal changes in tooth tip clearance can lead to nonlinear degradation in efficiency. Notably, a zero-clearance condition caused a transmission efficiency drop of up to 17%, due to increased friction and contact instability. This finding highlights the critical role of precision manufacturing and optimal clearance control in ensuring both performance and reliability.

These results generally follow the same trend as recent findings by Wang et al. [19], who demonstrated that even small adjustments in the pin tooth number and geometric ratios can significantly improve the dynamic transmission efficiency of cycloidal gear pairs. Their optimization study reported up to 29.9% reduction in power loss and a measurable decrease in vibration amplitude, highlighting the importance of clearance-sensitive design parameters in overall system performance.

4.5 Practical Implications

Collectively, these results affirm the utility of the proposed FEA-MBD framework in supporting iterative design and performance evaluation of cycloidal gear systems. The approach not only streamlines the modeling process through parameter automation but also provides actionable design insights, particularly in high-precision fields such as robotics, aerospace, and advanced mechatronic systems. Future work may incorporate thermal and wear modeling to further expand the framework's applicability.

5 CONCLUSION

This study presented a parametric simulation framework that integrates FEA and MBD to analyze the static and dynamic performance of cycloidal gear actuators. Through high-fidelity modeling and automated parameter control, the framework enabled quantitative evaluation of key geometric clearances and their influence on transmission efficiency.

Simulation results show that variations in pin-fit clearance have a relatively minor impact on efficiency - when the clearance between the cycloidal wheel pin and the output pin hole is reduced from 0.15 mm to 0.05 mm, the efficiency decreases by only 1%. In contrast, tooth tip clearance plays a much more critical role: reducing the clearance between internal and external cycloidal teeth to 0.075 mm and 0 mm resulted in efficiency losses of approximately 5% and 17%, respectively. This degradation is nonlinear and accelerates as clearance approaches zero, due to increased sliding, reduced force arms, and deteriorated load distribution.

These findings generally align with recent research by Zhang et al. [20], who demonstrated that geometric clearance and contact deformation significantly affect the efficiency, stiffness, and backlash of cycloidal gear systems. Their CDFM method further confirmed that tooth number and eccentric deviation introduce nonlinear losses in performance, underscoring the need for precise tolerance control. Moreover, Xu et al. [21] highlighted that long-term wear accumulation in pin teeth progressively increases

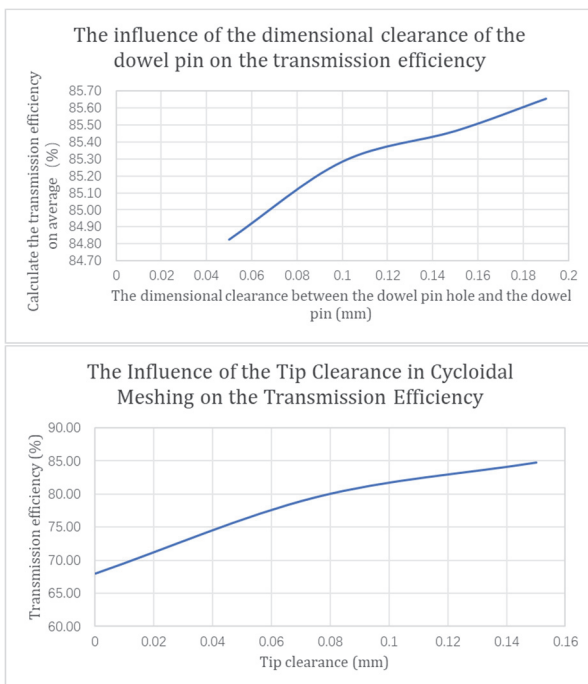


Figure 16 Impact curves of different pin-to-pin hole clearances and various internal and external cycloidal tooth tip clearances on average transmission efficiency

transmission error - particularly after 3000 hours of operation - emphasizing the importance of incorporating wear prediction in early-stage design.

Therefore, while small adjustments in pin fit can enhance compactness with minimal performance loss, tooth profile clearance must be strictly controlled. A minimum clearance of 0.075 mm is recommended to ensure meshing stability and avoid excessive power loss. High manufacturing accuracy in both tooth profile and eccentricity is essential to meet performance expectations.

The results confirm that the proposed configuration meets all key functional criteria: accurate transmission ratio, sufficient structural strength, and predicted service life for major components. In addition, the sensitivity analysis validates that tooth tip clearance has a nonlinear and substantial effect on efficiency, reinforcing the need for tolerance optimization in precision gear applications.

In conclusion, the proposed FEA-MBD simulation framework not only streamlines the modeling process through modular scripting but also provides actionable design insights for cycloidal gear optimization. Future work will expand the framework to incorporate thermal effects, wear mechanisms, and experimental validation, enhancing its applicability in real-world engineering scenarios.

6 REFERENCES

- [1] Mo, J., Gong, X., Luo, S., Fu, S., Chang, X., & Liao, L. (2023). Geometric design and dynamic characteristics of a novel abnormal cycloidal gear reducer. *Advances in Mechanical Engineering*, 15(3), 16878132231158895. <https://doi.org/10.1177/16878132231158895>
- [2] Gao, S., Zhang, Y., Li, T., Ding, X., Ji, S., & Cao, Z. (2024). Influence of cycloid pinwheel reducer structure parameters on transmission performance and optimized design with considering friction loss. *Optimization and Engineering*, 1-35. <https://doi.org/10.1007/s11081-024-09916-1>
- [3] Hosseinia, S. H., Manshoor, D., & Joudaki, J. (2024). Design and Finite Element Analysis of Cycloidal Gearboxes. *Mechanic of Advanced and Smart Materials*, 4(2), 238-255. <https://doi.org/10.61186/masm.4.2.238>
- [4] Tariq, H., Galym, Z., Amrin, A., & Spitas, C. (2024). Assessment of contact forces and stresses, torque ripple and efficiency of a cycloidal gear drive and its involute kinematical equivalent. *Mechanics Based Design of Structures and Machines*, 52(3), 1304-1323. <https://doi.org/10.1080/15397734.2022.2144885>
- [5] Zhang, Z., Zhao, S., & Zeng, M. (2023). Finite Element Dynamic Simulation and Fatigue Life Test Analysis of RV Reducer. *Academic Journal of Engineering and Technology Science*, 6(4), 58-62. <https://doi.org/10.25236/ajets.2023.060410>
- [6] Wang, C. & Mao, K. (2021). Design of high power density for RV reducer. *Journal of the Brazilian Society of Mechanical Sciences and Engineering*, 43(6), 291. <https://doi.org/10.1007/s40430-021-03011-7>
- [7] Zhang, R., Zhou, J., & Wei, Z. (2022). Study on transmission error and torsional stiffness of RV reducer under wear. *Journal of Mechanical Science and Technology*, 36(8), 4067-4081. <https://doi.org/10.1007/s12206-022-0727-0>
- [8] Jang, D. J., Kim, Y. C., Hong, E. P., & Kim, G. S. (2021). Geometry design and dynamic analysis of a modified cycloid reducer with epitrochoid tooth profile. *Mechanism and Machine Theory*, 164, 104399. <https://doi.org/10.1016/j.mechmachtheory.2021.104399>
- [9] Kurowski, P. M. (2022). *Finite element analysis for design engineers*. SAE International.
- [10] Jiang, X., Liao, H., Fan, D., & Zhang, S. (2019). An Angular Position-Based Two-Stage Friction Modeling and Compensation Method for RV Transmission System. *Tehnički vjesnik*, 26(6), 1720-1728. <https://doi.org/10.17559/tv-20190728151930>
- [11] Chen, Z. & Zhao, J. (2023). Bearing Fault Diagnosis Based on Wide Deep Convolutional Neural Network and Long Short Term Memory. *Tehnički vjesnik - Technical Gazette*, 30(1), 265-273. <https://doi.org/10.17559/TV-20220512135354>
- [12] Yang, M., Zhang, D., Cheng, C., & Han, X. (2021). Reliability-based design optimization for RV reducer with experimental constraint. *Structural and Multidisciplinary Optimization*, 63(4), 2047-2064. <https://doi.org/10.1007/s00158-020-02781-3>
- [13] Zhang, Y., Li, L., & Ji, S. (2022). Influence of cycloid-pin gear design parameters on bearing capacity and optimized design. *Journal of the Brazilian Society of Mechanical Sciences and Engineering*, 44(4), 123. <https://doi.org/10.1007/s40430-022-03426-w>
- [14] Yang, Y., Zhou, G., Chang, L., & Chen, G. (2021). A modelling approach for kinematic equivalent mechanism and rotational transmission error of RV reducer. *Mechanism and Machine Theory*, 163, 104384. <https://doi.org/10.1016/j.mechmachtheory.2021.104384>
- [15] Wang, F., He, Y., Wu, X., & Kang, M. (2022). Flow field characteristics and experimental research on inner-jet electrochemical face grinding of SUS420J2 stainless steel. *Scientific Reports*, 12(1), 11789. <https://doi.org/10.1038/s41598-022-16099-1>
- [16] Marques, S. C., Molter, D. L., Almeida, L. D. S., & dos Santos, D. S. (2024). The influence of the experimental methodology on evaluating the hydrogen embrittlement susceptibility of AISI 4340 steel manufactured by different routes. *Engineering Failure Analysis*, 162, 108361. <https://doi.org/10.1016/j.engfailanal.2024.108361>
- [17] Gao, S., Li, Y., Zhang, Y., Ji, S., & Wang, J. (2024). Lifespan Evaluation for a Standard RV Reducer based on Fatigue Strength Theory. *Strojniški vestnik-Journal of Mechanical Engineering*, 70(9-10), 452-565. <https://doi.org/10.5545/sv-jme.2023.897>
- [18] Tariq, H., Galym, Z., Amrin, A., & Spitas, C. (2024). Assessment of contact forces and stresses, torque ripple and efficiency of a cycloidal gear drive and its involute kinematical equivalent. *Mechanics Based Design of Structures and Machines*, 52(3), 1304-1323. <https://doi.org/10.1080/15397734.2022.2144885>
- [19] Wang, C. (2024). A study of the dynamic transmission efficiency of the cycloid pin gear pair under dynamic characteristic analysis. *Journal of Vibration and Control*, 10775463241296579. <https://doi.org/10.1177/10775463241296579>
- [20] Qi, L., Yang, D., Cao, B., Li, Z., & Liu, H. (2024). Design principle and numerical analysis for cycloidal drive considering clearance, deformation, and friction. *Alexandria Engineering Journal*, 91, 403-418. <https://doi.org/10.1016/j.aej.2024.01.077>
- [21] Xu, H., Wei, C., Gui, W., Yang, S., He, Y., Xie, G., & Wu, Y. (2024). Investigation of the impact of cycloidal gear pin tooth wear on transmission error in precision planetary cycloidal reducers. *International Journal of Metrology and Quality Engineering*, 15, 9. <https://doi.org/10.1051/ijmqe/2024007>

Contact information:

Feng MIAO, Master's student
School of Mechanical Engineering,
Dalian Jiao Tong University,
No. 794, Huanghe Road, Shahekou District, Dalian, Liaoning Province,
China
E-mail: 949207181@qq.com

Junhua BAO, Associate Professor
(Corresponding author)
School of Mechanical Engineering,
Dalian Jiao Tong University,
No. 794, Huanghe Road, Shahekou District, Dalian, Liaoning Province,
China
E-mail: 20794198@qq.com